01 Dec 2019

Magnetic Field Induced Ferrofluid Droplet Breakup in a Simple Shear Flow at a Low Reynolds Number

Md Rifat Hassan

Cheng Wang
Missouri University of Science and Technology, wancheng@mst.edu

Recommended Citation

M. R. Hassan and C. Wang, "Magnetic Field Induced Ferrofluid Droplet Breakup in a Simple Shear Flow at a Low Reynolds Number," *Physics of Fluids*, vol. 31, no. 12, American Institute of Physics Inc., Dec 2019. The definitive version is available at https://doi.org/10.1063/1.5124134

Physics of Fluids ARTICLE scitation.org/journal/phf

Magnetic field induced ferrofluid droplet breakup in a simple shear flow at a low Reynolds number

Cite as: Phys. Fluids 31, 127104 (2019); doi: 10.1063/1.5124134
Submitted: 12 August 2019 • Accepted: 22 November 2019 •
Published Online: 10 December 2019

Md Rifat Hassan and Cheng Wang (王成)[a]

AFFILIATIONS

Department of Mechanical and Aerospace Engineering, Missouri University of Science and Technology, 400 W. 13th St., Rolla, Missouri 65409, USA

[a]Electronic mail: wancheng@mst.edu

ABSTRACT

The breakup phenomenon of a ferrofluid droplet in a simple shear flow under a uniform magnetic field is numerically investigated in this paper. The numerical simulation, based on the finite element method, uses a level set method to capture the dynamic evolution of the droplet interface between the two phases. Focusing on small Reynolds numbers (i.e., Re ≤ 0.03), systematic numerical simulations are carried out to analyze the effects of magnetic field strength, direction, and viscosity ratio on the breakup phenomenon of the ferrofluid droplet. The results suggest that applying a magnetic field along $\alpha = 45^\circ$ and 90° relative to the flow direction initiates breakup in a ferrofluid droplet at a low capillary number in the Stokes flow regime, where the droplet usually does not break up in a shear flow alone. At $\alpha = 0^\circ$ and 135°, the magnetic field suppresses breakup. Also, there exists a critical magnetic bond number, Bo_{cr}, below which the droplet does not rupture, which is also dependent on the direction of the magnetic field. Additionally, the effect of the viscosity ratio on droplet breakup is examined at variable magnetic bond numbers. The results indicate a decrease in the critical magnetic bond number Bo_{cr} values for more viscous droplets. Furthermore, more satellite droplets are observed at $\alpha = 45^\circ$ compared to $\alpha = 90^\circ$, not only at higher magnetic field strengths but also at larger viscosity ratios.

I. INTRODUCTION

Droplet dispersion in another immiscible liquid is commonly experienced in a number of industrial applications that deal with cosmetics, food processing,[1] pharmaceutical design,[2] and polymer processing.[3–5] Most of these applications utilize highly concentrated emulsions, where the morphology of the dispersed phase component plays a crucial role in determining the physical and rheological properties of the emulsions. Consequently, these drop sizes become key to the design of processing equipment for certain emulsion properties and conditions, which is often complicated by the interplay between the flow field and fluid components behavior.[6,7]

When a droplet is subjected to shear flow, it deforms. Moreover, if the flow field exceeds a specific critical value, the droplet ruptures and gives rise to daughter droplets via a process called "elongative end pinching," which also reduces the mean size of the droplets.[8] Smaller sized droplets, having a larger total interfacial area, produce more stable emulsions and are considered a fundamental scaling parameter for a number of mass transfer and chemical reactions.[9] In the existing literature,[10] three different droplet breakup mechanisms (i.e., binary breakup, capillary breakup, and tipstreaming) are studied, but in this study we will restrict ourselves to binary breakup in a simple shear flow.

In binary breakup, the behavior of an isolated drop is mainly governed by two dimensionless numbers: The first one is known as the capillary number Ca, which denotes the competition between two forces: the viscous shear stress of the continuous phase $\eta_c\dot{\gamma}$ which causes deformation, and the Laplace pressure σ/R_0 which resists deformation, where η_c, $\dot{\gamma}$, σ, and R_0 represent the continuous phase viscosity, shear rate, interfacial tension, and initial radius of the droplet, respectively. The second one is the viscosity ratio $\lambda = \eta_d/\eta_c$, where η_d denotes the viscosity of the droplet phase. There exists a critical capillary number, Ca_{cr}, above which the droplet ruptures, and from the experimental analysis of Grace[11] it is realized that this critical capillary number is strongly

dependent on the viscosity ratio [i.e., $Ca_{cr} = f(\lambda)$]. The results show that an isolated droplet experiences rotational motion in a simple shear flow which eventually prevents the droplet from breakup at a higher viscosity ratio (i.e., $\lambda = 3.8$). Rumscheidt and Mason[12] also found that at $\lambda > 4$, the droplet initially tumbles and eventually turns into an ellipsoidal shape aligned with the flow direction.

Following the pioneering work of Taylor,[13,14] several numerical and theoretical investigations have been conducted to analyze droplet breakup in emulsification and mixing.[15–19] Li *et al.*[20] performed a numerical simulation on the breakup mechanism of a viscous droplet in a simple shear flow and found that it is possible to induce droplet breakup at a low capillary number in the Stokes flow with an increased Reynolds number. Debruijn[10] built a Couette device with the aim to investigate the breakup phenomena of non-Newtonian droplets in a quasisteady simple shear flow. Barthes-Biesel and Acrivos[21] studied the breakup conditions of a liquid droplet freely suspended in a linear shear field and observed that the droplet yields a burst criterion for λ ranging between 0.1 and 3.6. De Menech[22] numerically examined droplet breakup in a three dimensional T-shaped junction and observed that the critical capillary number at which the droplet experiences breakup is related to the viscosity ratio. Also, a two-dimensional numerical study on droplet deformation and breakup has been performed by van der Sman and van der Graaf[23] using the lattice Boltzmann model.

In experimental analyses, breakup of a solitary drop is usually investigated either by direct observation of a droplet in a flow field or by observing the change in droplet size distribution. Sibilo *et al.*[24] studied the effect of the matrix elasticity on the breakup of an isolated Newtonian drop in a shear flow and concluded that matrix elasticity hinders breakup in a droplet. Vananroye *et al.*[25] conducted experiments on droplet breakup in sheared emulsions and found that, even at $\lambda > 4$, it is possible to induce breakup in droplets by applying a shear field to a larger confinement. Furthermore, an experimental study on the droplet formation and breakup in a microfluidic T-junction has been done by Garstecki *et al.*[26] and Leshansky and Pismen.[27]

In addition to hydrodynamic forces, external force fields (i.e., electric or magnetic fields) can also manipulate the overall rheology of the droplets.[28,29] Taylor[30] performed both theoretical and experimental investigation on the disintegration of water droplets in an electric field, while Collins *et al.*[31] performed simulations and experiments to investigate the mechanisms of cone formation, jet emission, and breakup of charged drops under the presence of an electric field. Also, the deformation and breakup of aqueous drops under large electric fields have been experimentally investigated by Eow and Ghadiri,[32] which shows that initial drop sizes greatly influence the magnitude of the electric field strength for the onset of droplet stability. Interestingly, instead of using electric and magnetic fields as an external means of manipulation, an alternative algorithm approach based on logic operations has been adopted to control droplets in a parallel manner by Katsikis *et al.*[33] Moreover, an excellent experimental study on the manipulation of droplets under electric fields in microfluidic devices has been performed by Link *et al.*[34]

A magnetic field can also be used to manipulate the shape of a droplet;[35] however, magnetic manipulation requires either the droplet or continuous phase to be a ferrofluid—a dispersion of magnetic nanoparticles (diameter typically around 10 nm and volume fraction about 5%). Due to the presence of magnetic properties, additional Maxwell stresses occur at the fluid-fluid interface in addition to the hydrodynamic stresses. Ferrofluid droplets involved in multiphase flows have notable biomedical applications in the treatment of retinal detachment,[36] and the ease of both integration and flexibility of operation render a magnetic field as a popular means of droplet manipulation in microfluidic devices. Banarjee *et al.*[37] investigated the behavior of confined ferrofluid droplets under weak magnetic fields applied in a direction parallel to the direction of the computational domain. Varma *et al.*[38] experimentally studied the merging of ferrofluid droplets under uniform magnetic fields on a lab-on-a-chip platform and also developed a micro-magnetofluidic numerical model to explain the ferrofluid droplet behavior in both uniform and hybrid magnetic fields.[39] Also, an investigation on the manipulation of ferrofluid droplets by a permanent magnetic field has been carried out by Ray *et al.*[40] Moreover, a thorough analysis on the controlled deformation and orientation of a ferrofluid droplet in a simple shear flow by means of a uniform magnetic field is presented in our recent work.[41]

However, the existing studies in the literature are mainly focused on the breakup of droplets in external flow conditions.[11,42,43] Recently, Cunha *et al.*[44] numerically studied magnetic field induced droplet breakup in shear flows at a higher Reynolds number (i.e., Re = 1). Their results suggest that when a magnetic field acts in a direction parallel to the direction of the flow field, it delays the breakup process and reduces the size of the satellite droplets. Instead, if the magnetic field is applied in a direction perpendicular to the flow direction, droplet breakup can be induced, delayed, or even prevented through some adjustments in magnetic field intensities. But until now, as per our knowledge, no one has ever studied the breakup mechanism of a droplet in a Stokes flow at low capillary numbers (where a droplet usually does not breakup) under the effect of magnetic fields, which is more applicable to a range of different microfluidic applications.[45–49] Also, a comprehensive study on the effect of the viscosity ratio on droplet breakup in shear flows under a uniform magnetic field is missing in the literature. Therefore, in this paper, we focus on investigating the effect of a uniform magnetic field on the droplet breakup phenomenon at the Stokes flow limit in a simple shear flow along some specific directions. Here, a two-dimensional (2D) simulation model is chosen in order to study a wide range of parameters, including magnetic field strength, direction, and viscosity ratio. Prior studies show that 2D numerical models are capable of qualitatively and correctly capturing the deformation of a ferrofluid droplet under a uniform magnetic field with great computational efficiency.[41,50] Our numerical model, based on a commercial FEM solver, is implemented to model the droplet interface by using the level set method and coupling the magnetic and flow fields.

The rest of the paper is categorized as follows: the numerical model is described in Sec. II. In Sec. III, we present the numerical and mathematical methods that are required to solve our computational model. In Sec. IV, we first validate our results against the existing theories in the literature and then examine the effect of the magnetic field strength and viscosity ratio on the droplet breakup phenomenon at different magnetic field directions. Finally, the major findings are summed up in Sec. V.

II. NUMERICAL MODEL

Figure 1 depicts the motion of a viscous, neutrally buoyant ferrofluid droplet dispersed in another viscous fluid medium, bounded by two plane walls translating in opposite directions and subjected to a uniform magnetic field, $\mathbf{H}_0$. Initially, the density and viscosity of both the phases are treated equal to each other (i.e., $\rho_c = \rho_d$ and $\eta_c = \eta_d$). The magnetic susceptibility of the ferrofluid droplet is considered 1 ($\chi_d = 1$), while the continuous phase is treated as a non-magnetic fluid medium ($\chi_c = 0$). The magnitude of the coefficient of the interfacial tension σ is considered equal to 0.0135 N/m.

Placing the ferrofluid droplet initially at the center, a simple shear flow with a constant shear $\dot{\gamma}$ is generated by moving the top wall of the computational domain with a velocity $\mathbf{u}_t = \frac{1}{2}\dot{\gamma}H_d\mathbf{e}_x$, while the bottom wall of the domain moves with a velocity of the same magnitude as the top wall, but in the opposite direction (i.e., $\mathbf{u}_b = -\frac{1}{2}\dot{\gamma}H_d\mathbf{e}_x$). The velocity is continuous at the interface of the droplet although the surface force experiences a discontinuity at the droplet interface due to the surface tension effect. The droplet also experiences a symmetric flow field with respect to its initial position, while the velocity is zero along the center line of the flow domain. In order to simulate infinite periodicity in the x-direction, a periodic flow condition is implemented not only at the left wall but also at the right wall of the flow domain. The application of a uniform magnetic field, $\mathbf{H}_0$, along different directions of the flow domain is denoted by the angle α. When the droplet undergoes deformation, the deformation is determined using the largest major-axis and smallest minor-axis dimensions, which are denoted by L and B, respectively. The orientation angle, defined by θ, is measured as the angle between the positive x-direction and the major axis of the droplet in a counterclockwise direction.

III. NUMERICAL SIMULATION METHOD

A. Level set method

In the study of droplet motion in a shear induced flow, most of the problems arise in tracking the free interface of the droplet, which moves to different locations following severe deformation including breakup. Therefore, in our model, an Euler approach based conservative level set method is implemented to solve the dynamically evolving droplet interface between the two fluid phases. The level set method uses a smeared Heaviside scalar function ϕ to distinguish the two fluid phases, and the value of ϕ undergoes a smooth transition between 0 and 1 across the interface. In the droplet phase, the value of ϕ is considered 1, while it is zero in the continuous phase. The interface of the droplet is defined by the 0.5 isocontour of ϕ. The level set function ϕ moves with the velocity of fluid $\mathbf{u}$ through the following equation:[51]

$$\frac{d\phi}{dt} + \mathbf{u}\cdot\nabla\phi = \gamma\nabla\cdot\left(\epsilon\nabla\phi - \phi(1-\phi)\frac{\nabla\phi}{|\nabla\phi|}\right). \tag{1}$$

In the above equation, ϵ is a parameter used to define the droplet interface thickness, and its magnitude equals half the largest mesh size of the region passed by the droplet in the domain. However, during the pinching stage, when the value of ϵ encounters a mesh size less than half of the largest mesh size in the pinching region, it fails to resolve the interface of the droplet and eventually initiates a breakup in the middle. In our study, the magnitude of the largest mesh element size is considered equal to 4% of the diameter of the droplet, and using a mesh size lower than 4% of the droplet diameter generates a similar type of breakup phenomenon with reasonably identical shaped droplets; however, a slight increase in the breakup time is observed with the decrease in the largest mesh size. On the other hand, the re-initialization parameter γ needs a careful tuning for specific problems since too small or too high values of γ can give rise to numerical instabilities and incorrect interface, respectively. In general, the maximum magnitude of the velocity observed in the flow domain is considered an optimum value for the re-initialization parameter γ. Also, the unit normal to the interface $\mathbf{n}$ can be calculated using the level set function as

$$\mathbf{n} = \frac{\nabla\phi}{|\nabla\phi|}. \tag{2}$$

The level set method usually considers the multiphase flows as a single phase flow, where the level set value ϕ smoothen the jump of different parameters, such as density (ρ), magnetic permeability (μ), dynamic viscosity (η), and magnetic susceptibility (χ), across the droplet interface through the following equations:

$$\rho = \rho_c + (\rho_d - \rho_c)\phi, \qquad \mu = \mu_c + (\mu_d - \mu_c)\phi, \tag{3}$$

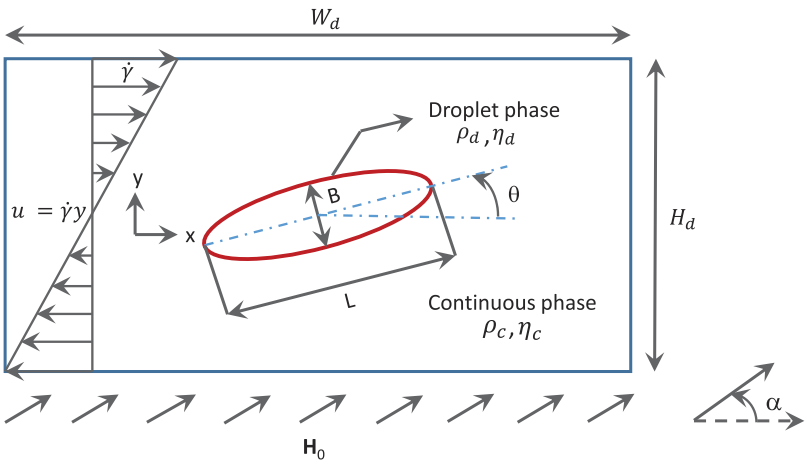

FIG. 1. Schematic of the computational domain, including a ferrofluid droplet dispersed in another fluid medium in a simple shear flow subjected to a uniform magnetic field, $\mathbf{H}_0$.

$$\eta = \eta_c + (\eta_d - \eta_c)\phi, \qquad \chi = \chi_c + (\chi_d - \chi_c)\phi, \tag{4}$$

where the continuous phase and droplet phase are represented by the subscripts c and d, respectively.

B. Governing equations

The incompressible laminar fluid flow motion, involving a viscous ferrofluid droplet suspended in another viscous fluid, can be described by the time-dependent Navier-Stokes equations, which are defined as follows:

$$\nabla \cdot \mathbf{u} = 0 \tag{5}$$

and

$$\rho\left(\frac{\partial \mathbf{u}}{\partial t} + \mathbf{u} \cdot \nabla \mathbf{u}\right) = -\nabla p + \nabla \cdot \boldsymbol{\tau} + \mathbf{F}_\sigma + \mathbf{F}_m. \tag{6}$$

Equations (5) and (6) also obey the law of conservation of mass and momentum, and the symbols p and $\boldsymbol{\tau}$ denote pressure and viscous stress, while the surface tension and magnetic forces are represented by $\mathbf{F}_\sigma$ and $\mathbf{F}_m$, respectively.

Again, the viscous stress tensor equals to $\eta\left[(\nabla \mathbf{u}) + (\nabla \mathbf{u})^T\right]$, and the surface tension force $\mathbf{F}_\sigma$ can be related to the coefficient of surface tension σ through the following equation:

$$\mathbf{F}_\sigma = \nabla \cdot [\sigma\{\mathbf{I} + (-\mathbf{n}\mathbf{n}^T)\}\delta], \tag{7}$$

where $\mathbf{I}$ is the identity operator and δ is the Dirac delta function, which can also be approximated by the level set function ϕ as

$$\delta = 6|\phi(1-\phi)||\nabla\phi|. \tag{8}$$

Also, the additional magnetic stresses generated due to the application of a uniform magnetic field can be represented by the magnetic stress tensor $\boldsymbol{\tau}_m$, which is eventually required to calculate the applied magnetic force $\mathbf{F}_m$ in the computational domain. The calculation of the magnetic force $\mathbf{F}_m$ is as follows:[52]

$$\mathbf{F}_m = \nabla \cdot \boldsymbol{\tau}_m = \nabla \cdot \left(\mu \mathbf{H}\mathbf{H} - \frac{\mu}{2} H^2 \mathbf{I}\right), \tag{9}$$

where μ is the permeability of the fluid that varies according to the level set function ϕ, and $H^2 = |\mathbf{H}|^2$. A comprehensive understanding of the Maxwell equations and the constitutive relations among magnetic induction $\mathbf{B}$, magnetic field $\mathbf{H}$, and magnetization $\mathbf{M}$ is necessary for the calculation of magnetic stress tensor $\boldsymbol{\tau}_m$, which also maintain the following relationships:[53]

$$\nabla \times \mathbf{H} = 0, \quad \mathbf{M} = \chi \mathbf{H}, \quad \nabla \cdot \mathbf{B} = 0,$$

and

$$\mathbf{B} = \mu_0(\mathbf{H} + \mathbf{M}) = \mu_0(1 + \chi)\mathbf{H}. \tag{10}$$

The symbol μ_0 denotes the permeability of vacuum, which is equal to $4\pi \times 10^{-7}$ N/A^2. A scalar magnetic potential ψ is defined under the consideration that it follows the relation $\mathbf{H} = -\nabla\psi$, which ultimately leads to the following equation:

$$\nabla \cdot (\mu \nabla \psi) = 0. \tag{11}$$

Moreover, in order to have a better understanding of the parameters that govern the overall dynamics of droplets, we rewrite the governing equations in terms of dimensionless groups. To achieve this, the droplet radius in the initial condition (R_0) is used as a scaling parameter for the length, whereas the time is scaled by the inverted shear rate $\frac{1}{\dot{\gamma}}$. The scaling for the nondimensionalization of other parameters is as follows:

$$p^* = \frac{p}{\eta\dot{\gamma}}, \quad \eta^* = \frac{\eta}{\eta_c}, \quad \rho^* = \frac{\rho}{\rho_c}, \quad \mu^* = \frac{\mu}{\mu_0}, \quad \mathbf{H}^* = \frac{\mathbf{H}}{H_0},$$

where H_0 is a scaling parameter that denotes the magnitude of the magnetic field $\mathbf{H}_0$ applied along different directions. Now, the Navier-Stokes equations in nondimensionalized form can be written as follows:

$$\nabla^* \cdot \mathbf{u}^* = 0, \tag{12}$$

$$\mathrm{Re}\left(\rho^* \frac{D\mathbf{u}^*}{Dt^*}\right) = -\nabla^* p^* + \nabla^* \cdot \tau^* + 2\frac{\mathrm{Bo}_m}{\mathrm{Ca}} \nabla^* \cdot \boldsymbol{\tau}_m^* + \frac{1}{\mathrm{Ca}} \mathbf{F}_\sigma^*. \tag{13}$$

In Eqs. (12) and (13), the asterisk ($*$) represents the nondimensional variables, and Ca, Re, and Bo$_m$ represent the capillary number, Reynolds number, and magnetic bond number, respectively, which can be elucidated as follows:

$$\mathrm{Ca} = \frac{\eta_c R_0 \dot{\gamma}}{\sigma}, \tag{14}$$

$$\mathrm{Re} = \frac{\rho_c {R_0}^2 \dot{\gamma}}{\eta_c}, \tag{15}$$

and

$$\mathrm{Bo}_m = \frac{R_0 \mu_0 {H_0}^2}{2\sigma}. \tag{16}$$

Several other important nondimensional groups, such as the viscosity ratio λ and permeability ratio ζ can be written as follows:

$$\lambda = \frac{\eta_d}{\eta_c} \quad \text{and} \quad \zeta = \frac{\mu_d}{\mu_0}. \tag{17}$$

Keeping the flow field restricted to the Stokes flow regime (i.e., Re $\lesssim$ 0.03), in this paper, the effects of different dimensionless groups Ca, Bo$_m$, λ, including α on the breakup phenomenon of the droplet will be investigated.

IV. RESULTS AND DISCUSSIONS

A. Droplet deformation in the high limit of shear flow (Ca ≥ 0.35)

At a small Reynolds number (i.e., Re ≤ 0.03), the flow is governed by Stokes flow equations. When a droplet is subjected to a simple shear flow, it deforms. According to Taylor,[13,14] the deformation of a neutrally buoyant, viscous droplet suspended in another viscous medium under a simple shear flow at the Stokes flow limit can be defined as

$$D_{taylor} = \frac{L - B}{L + B} = \frac{19\lambda + 16}{16\lambda + 16}\mathrm{Ca}. \tag{18}$$

Taylor formulated the above equation assuming that the shear flow is unbounded with a vanishing Reynolds number; however, in numerical studies, a simple shear flow is usually generated by two plane walls translating in opposite directions, which gives rise to the so-called confinement effect. This confinement effect, characterized

by the confinement ratio $\frac{2R_0}{H_d}$, has a negligible effect on the deformation of the droplet when $\frac{2R_0}{H_d} < 0.4$.[54,55] In our case, the confinement ratio is equal to 0.1, and therefore, the confinement effect can be neglected. In this section, we study the evolution of equilibrium droplet shapes in the high limit of shear flow under the Stokes flow regime and then compare the numerical results against the existing theories in the literature.

Figure 2 represents the time evolution of droplet deformation parameter D and the corresponding equilibrium droplet shapes at different capillary numbers. From Fig. 2(a), it can be seen that as the shear rate increases, the deformation increases. Also, it takes a very small amount of computational time to reach the steady state deformation. Moreover, we compared our numerical results against the asymptotic theory for small deformation given by Cox.[56] According to Cox, the deformation of a droplet can be approximated as follows:

$$D_{cox} = D_{taylor}\left[1 + \left(\frac{19\mathrm{Ca}\lambda}{20}\right)^2\right]^{-\frac{1}{2}}, \tag{19}$$

where D_{taylor} is the Taylor deformation parameter defined in Eq. (18). From Fig. 2(b), it can be inferred that the numerical results are in very good agreement with the Cox deformation theory. Even for the maximum shear rate considered in our study (i.e., Ca = 0.5), the error between the numerical and theoretical results is found to be approximately 3.5%.

Furthermore, the corresponding equilibrium droplet shapes are shown in Fig. 2(c). The droplet shapes reveal that with an increasing capillary number, the droplet is more stretched toward the direction of the flow field, which is also consistent with our previous findings.[41] The droplet experiences maximum shear stress along its poles. Also, the velocity field acts tangentially at the droplet interface, and near the droplet, the flow field follows the curvature of the droplet, which is also consistent with the free surface conditions. A closed circulation is observed inside the droplet due to the competition between the surface tension driven flow and the flow field outside the droplet, which is represented by the arrow in the velocity fields.

Moreover, we performed simulations at higher Reynolds numbers (i.e., Re = 1) to verify that our numerical model is capable of capturing droplet breakup at higher Reynolds numbers. Figure 3 shows the transformation of an ellipsoidal droplet into multiple droplets following a breakup at Re = 1, Ca = 0.5, and λ = 1.2. These droplet breakup results agree well with the findings of Cunha *et al.*,[44] except the fact that in their case, one satellite droplet was

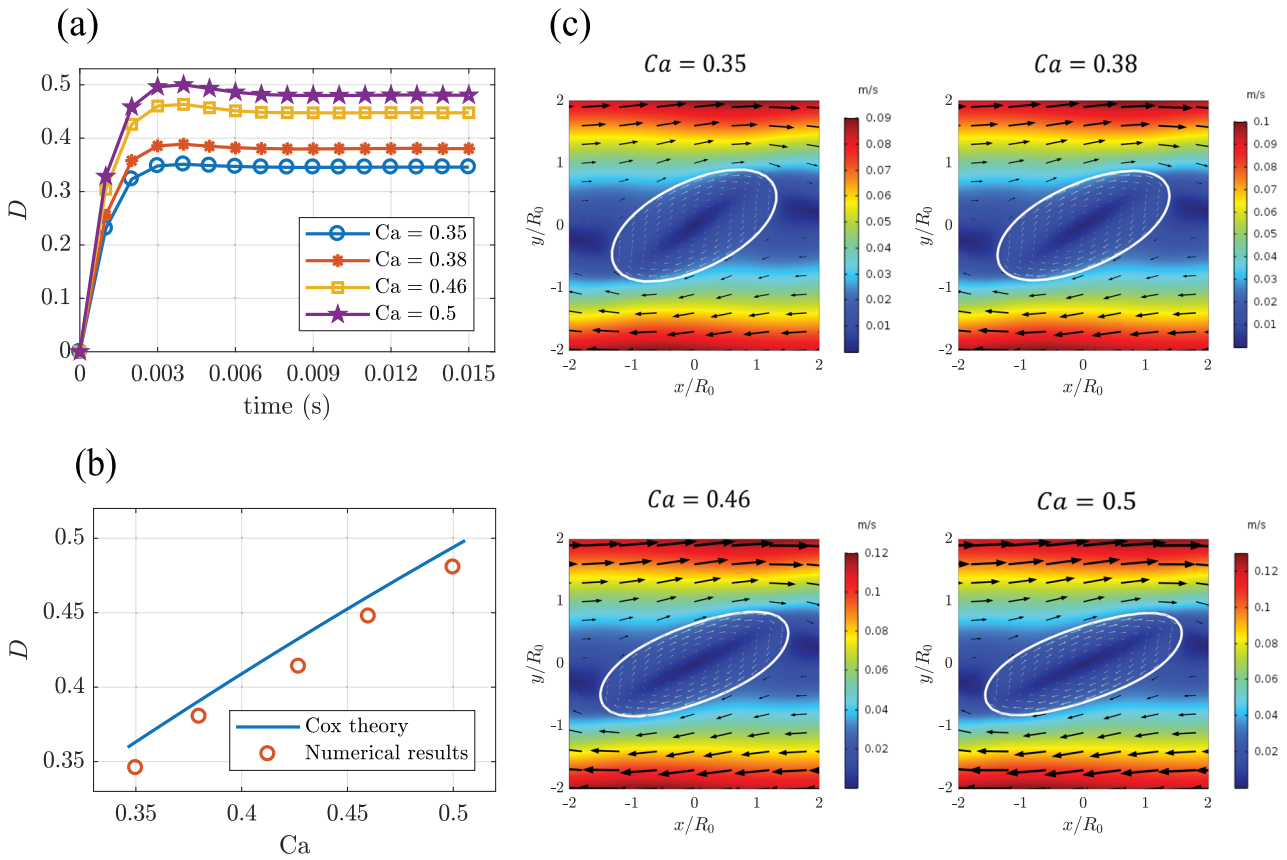

FIG. 2. Droplet deformation in the high limit of shear flow. (a) D vs time; (b) comparison of numerical results against the Cox theory;[56] and (c) equilibrium shape of the droplet.

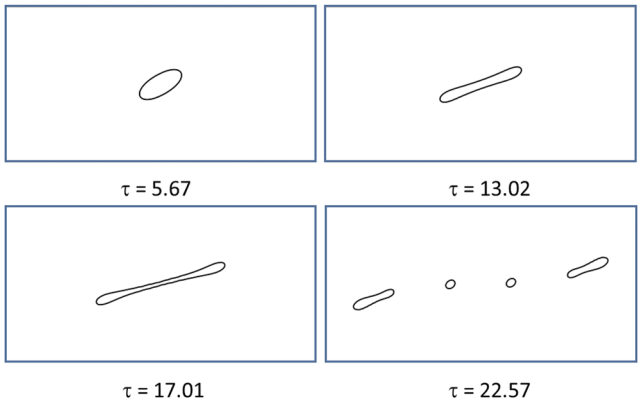

FIG. 3. Droplet breakup in a simple shear flow at Re = 1, Ca = 0.5, and λ = 1.2.

observed, while in our numerical model, we observed two satellite droplets after the breakup. The primary reason behind this phenomenon can be attributed to the resolution of the interface thickness of the droplet, i.e., in their numerical model the interface thickness was considered 1.5 times the largest mesh element size h ($\epsilon = 1.5h$), whereas in our study, a better interface resolution is considered ($\epsilon = 0.5h$). Additionally, the validation of the droplet deformation results under the influence of uniform magnetic fields against the findings of Afkhami *et al.*[57] is presented in our previous work.[41]

B. Droplet breakup under the effect of the magnetic field

When applied, an external magnetic field can significantly affect the deformation and orientation of a ferrofluid droplet, which in turn offers the possibility of controlling the emulsion rheology of a droplet by inducing or suppressing the topological changes of the suspended droplet in a simple shear flow. The existing studies in the literature show that it is possible to induce breakup at a low capillary number in a Stokes flow (where the droplet does not break) by increasing the Reynolds number.[20] Recently, Cunha *et al.*[44] have studied field induced droplet breakup in a shear flow at a higher Reynolds number where the magnetic field is applied in a perpendicular and parallel direction to the flow field. In this section, at a fixed viscosity ratio (i.e., λ = 1) and capillary number (i.e., Ca = 0.45), we study the effect of an external uniform magnetic field on the rupture of a ferrofluid droplet in the Stokes flow regime along some specific directions. Also, note that in the absence of any external forces (i.e., $\mathrm{Bo}_m = 0$), at Ca = 0.45 and λ = 1, the orientation angle of the droplet is found to be approximately 21.9°. In the remaining portion of the study, the Reynolds number is considered 0.03 (i.e., Re = 0.03).

1. α = 45°

Figure 4 represents the effect of a uniform magnetic field on the droplet rheology in a simple shear flow at α = 45°. From Fig. 4(a), it can be seen that as the magnetic field strength increases, the deformation D of the ferrofluid droplet increases. The droplet shape also attains a steady state within a very small amount of computational time; however, at a magnetic bond number equal to 2.09 (i.e., Bo_m = 2.09), the droplet deformation shows an unsteady behavior for a longer period of time and reaches a steady state around 0.02 s. Furthermore, as we continue increasing the magnetic bond number beyond 2.69 (i.e., $\mathrm{Bo}_m \geq 2.69$), the droplet deforms even more without reaching a steady state, and this unsteady behavior ultimately initiates the breakup. The sudden decline in the droplet deformation in Fig. 4(a) denotes that a breakup has been initiated by the external magnetic field. Also, at α = 45° we found the critical deformation (deformation at which the droplet disintegrates) to be approximately 0.87, i.e., $D_{cr} \approx 0.87$. Additionally, the droplet is found to rupture earlier under a higher magnetic field strength, i.e., Bo_m = 3.72. Figure 4(b) displays the estimated rupture time τ_b as a function of magnetic bond number Bo_m, which clearly indicates that τ_b follows a nonlinear relationship with Bo_m. As the intensity of magnetic field increases, the droplet ruptures even quicker. These results also demonstrate that at α = 45°, a critical magnetic bond number exists below which the droplet does not break up anymore, and the numerical simulations suggest this value to be approximately 2.23 (i.e., $\mathrm{Bo}_{cr} \approx 2.23$).

Figure 5 shows the evolution of droplet breakup over time at different magnetic bond numbers, Bo_m. From Fig. 5(b), it can be seen that as time proceeds, the droplet transforms into a dumbbell shape from an ellipsoidal shape along with the bulbs at the ends of the droplet with a fixed diameter. As the droplet stretches itself

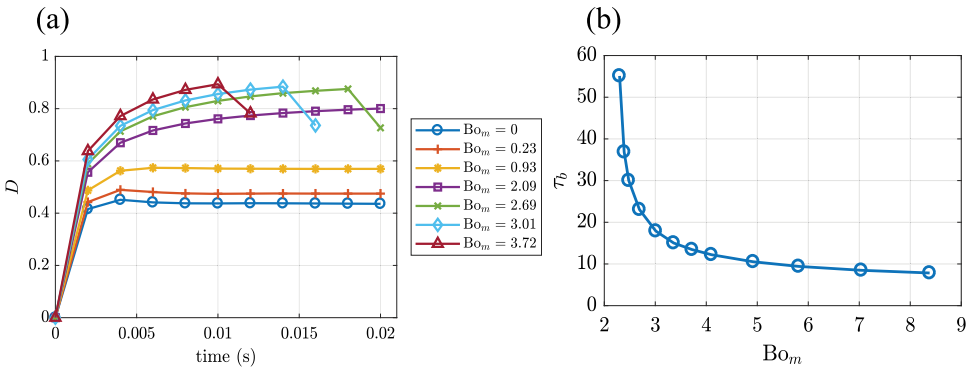

FIG. 4. Droplet under the effect of a magnetic field in a simple shear flow at 45° (i.e., α = 45°), Ca = 0.45, and λ = 1. (a) D vs time; (b) droplet breakup time, τ_b vs Bo_m.

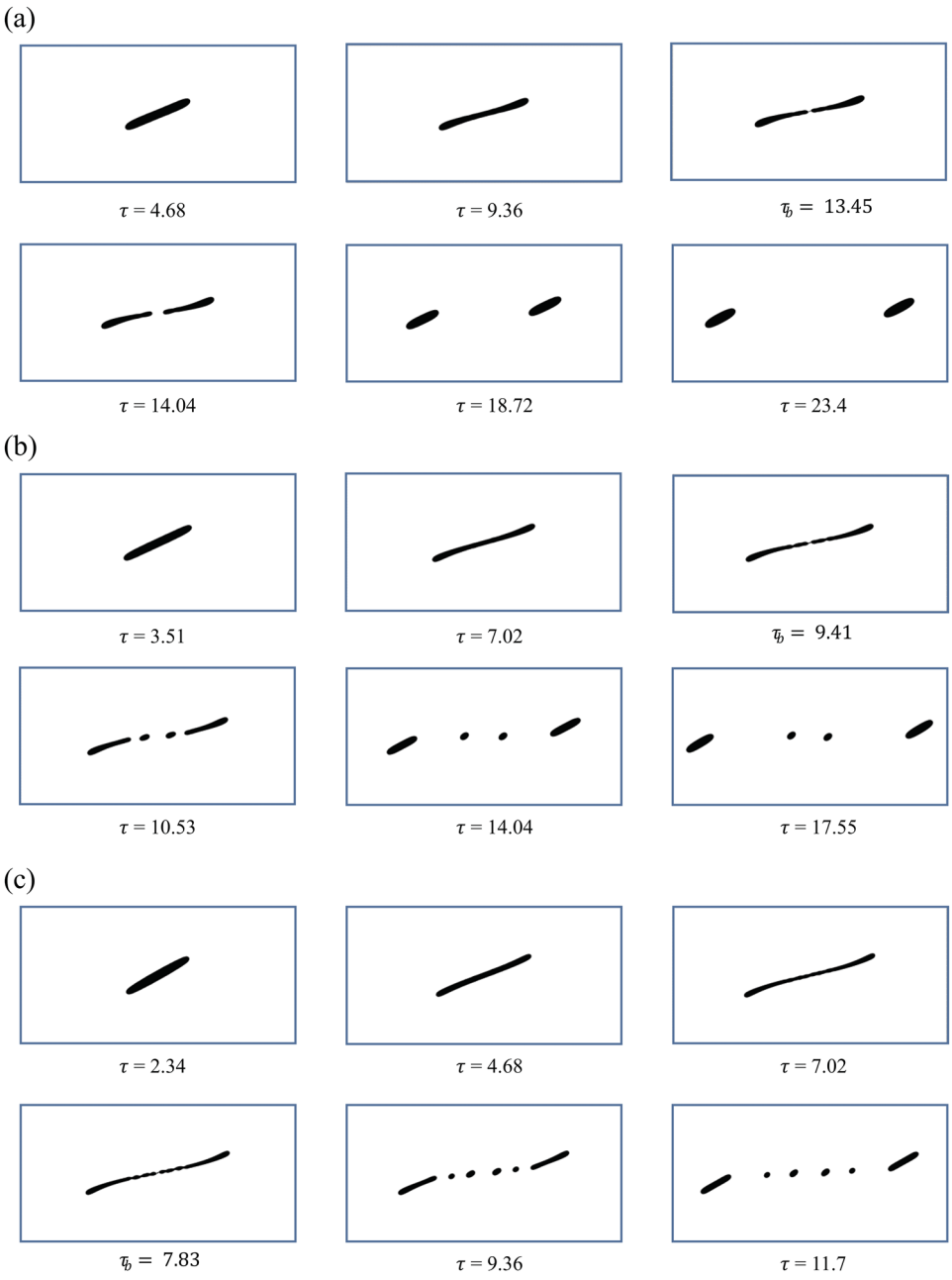

FIG. 5. Evolution of droplet breakup under the magnetic field effect in a simple shear flow at 45° (i.e., $\alpha = 45°$), Ca = 0.45, and $\lambda = 1$. (a) $Bo_m = 3.72$; (b) $Bo_m = 5.81$; and (c) $Bo_m = 8.38$.

toward the direction of the flow field, a neck is developed at the center of the droplet that continuously thins over time. In this case, the magnetic field aids the droplet more in stretching toward the flow field direction. Moreover, due to the presence of circulation inside the bulbous ends of the droplet, the surface tension driven flow acts stronger near the bulbous end while the flow is much weaker near the neck. As a result, this unstable neck eventually leads to ends pinching off ($\tau_b = 9.41$) and gives rise to satellite droplets with the remaining liquid thread in the middle; however, at $Bo_m = 3.72$ [Fig. 5(a)], we observed an eventual breakup of the mother droplet into two daughter droplets. Now, as we go on increasing the magnetic field strength (i.e., $Bo_m = 8.38$), multiple satellite droplets appear in the computational domain. Interestingly, from Fig. 5(c) we can see that the size of the second pair of satellite droplets seems smaller compared to the first pair of satellite droplets. According to Marks,[58] if the original volume fraction is not totally used by

the breakup process for a large droplet, the ends of the remaining volume fraction will go through a similar breakup process as before and give rise to another pair of smaller satellite droplets, and our results agree very well with the experimental observations of Marks.[58]

2. $\alpha = 90°$

Now, we apply the magnetic field at an angle $\alpha = 90°$ to observe its effect on the breakup phenomenon of the droplet suspended in a shear flow. Figure 6(a) displays the evolution of deformation parameter D over time when the magnetic field is applied at an angle $\alpha = 90°$. It can be seen that with the increase in magnetic field strength, deformation D increases and reaches a steady state around 0.008 s; although at $\mathrm{Bo}_m = 3.01$, the droplet starts to show unsteady behavior. Moreover, as we continuously increase the magnetic field strength to $\mathrm{Bo}_m = 3.72$, similar to the case mentioned above, we observe the first breakup where the mother droplet breaks into two daughter droplets. In this case, the critical deformation is found to be approximately 0.85 (i.e., $D_{cr} \approx 0.85$). Also, at $\alpha = 90°$ the first breakup is seen at a magnetic bond number, $\mathrm{Bo}_m = 3.72$, which is slightly above the magnetic bond number that is required to initiate the first breakup at $\alpha = 45°$ (i.e., $\mathrm{Bo}_m = 2.69$). The primary reason behind this fact is that at $\alpha = 45°$, the magnetic field aids the droplet in stretching in the same direction as the velocity field, which in turn initiates the droplet breakup faster. Figure 6(b) illustrates the relationship between the droplet breakup time, τ_b, and magnetic bond number, Bo_m, and the numerical results suggest that the critical magnetic bond number in this case lies around 3.63 (i.e., $\mathrm{Bo}_{cr} \approx 3.63$).

Figure 7 demonstrates the evolution of droplet shapes under the magnetic field effect at $\alpha = 90°$, and it shows that the droplet continuously deforms and eventually breaks up at some point; however, no satellite droplets are observed until we apply a magnetic field strength that corresponds to a magnetic bond number, $\mathrm{Bo}_m = 8.38$ [Fig. 7(c)]. In all these cases, the droplet follows a similar type of evolution from the initial stage to the breakup stage as described in Sec. IV B 1 (i.e., the droplet stretches itself from spherical to the dumbbell shape followed by an ellipsoidal shape, then the ends pinch off due to the presence of instabilities at the central portion, which in turn generate multiple droplets). Interestingly, in Fig. 7(c) fewer satellite droplets appear compared to the number of satellite droplets that we observed at $\alpha = 45°$ [Fig. 5(c)] for the same magnitude of magnetic field strength (i.e., $\mathrm{Bo}_m = 8.38$). The reason behind this could be attributed to the fact that in this case, the magnetic stress acts in a direction perpendicular to the flow field while the hydrodynamic stress acts along 45°, and the competition between hydrodynamic and magnetic stresses along two different directions results in a few number of necks along the droplet interface, which in turn produces fewer satellite droplets.

3. $\alpha = 0°$

Figure 8 represents the effect of the magnetic field on the droplet shape in a simple shear flow at $\alpha = 0°$. From Fig. 8(a), it can be seen that initially as the magnetic field strength increases up to $\mathrm{Bo}_m = 2.09$, the magnetic field has negligible effect on the deformation of the droplet since up to this point the shear flow is dominant and controls the deformation of the droplet. However, as the magnetic field strength starts to increase beyond $\mathrm{Bo}_m \geq 3.72$, the magnetic field tends to become dominant, and as a result the deformation of the droplet D increases and reaches a steady state within a very small amount of computational time. Figure 8(b) portrays the outline of the equilibrium droplet shapes at different magnetic bond numbers, Bo_m. The droplet shapes reveal that with the increase in magnetic field strength, the droplet aligns itself more toward the direction of the magnetic field with greater deformation. Even at a higher magnetic bond number, i.e., $\mathrm{Bo}_m = 8.38$, we did not observe any breakup. The primary reason behind this phenomenon is that with the increase in magnetic field strength, the magnetic field rotates the droplet from the extensional quadrant to the compressional quadrant of shear, and as a result the droplet is now so aligned with the flow direction that the shear stress is not strong enough to induce rupture, which also acts as a restorative mechanism of the droplet shape.

4. $\alpha = 135°$

Finally, we apply the magnetic field along 135° (i.e., $\alpha = 135°$) to understand its effect on the droplet deformation in a significantly strong shear flow. Figure 9 represents the droplet deformation behavior under a uniform magnetic field in a shear flow at $\alpha = 135°$. From Fig. 9(a), we can see that as the magnetic field strength gradually increases, the droplet deformation D decreases. This happens because, on the one hand, the shear flow is trying to deform

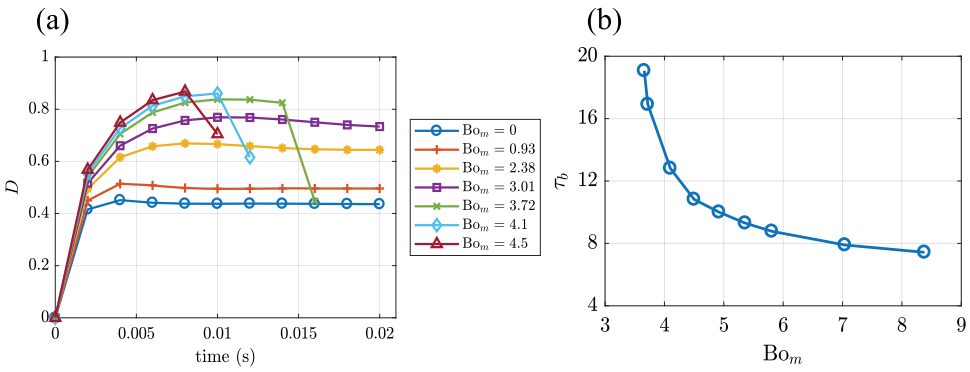

FIG. 6. Droplet under the effect of a magnetic field in a simple shear flow at 90° (i.e., $\alpha = 90°$), Ca = 0.45, and $\lambda = 1$. (a) D vs time; (b) droplet breakup time, τ_b vs Bo_m.

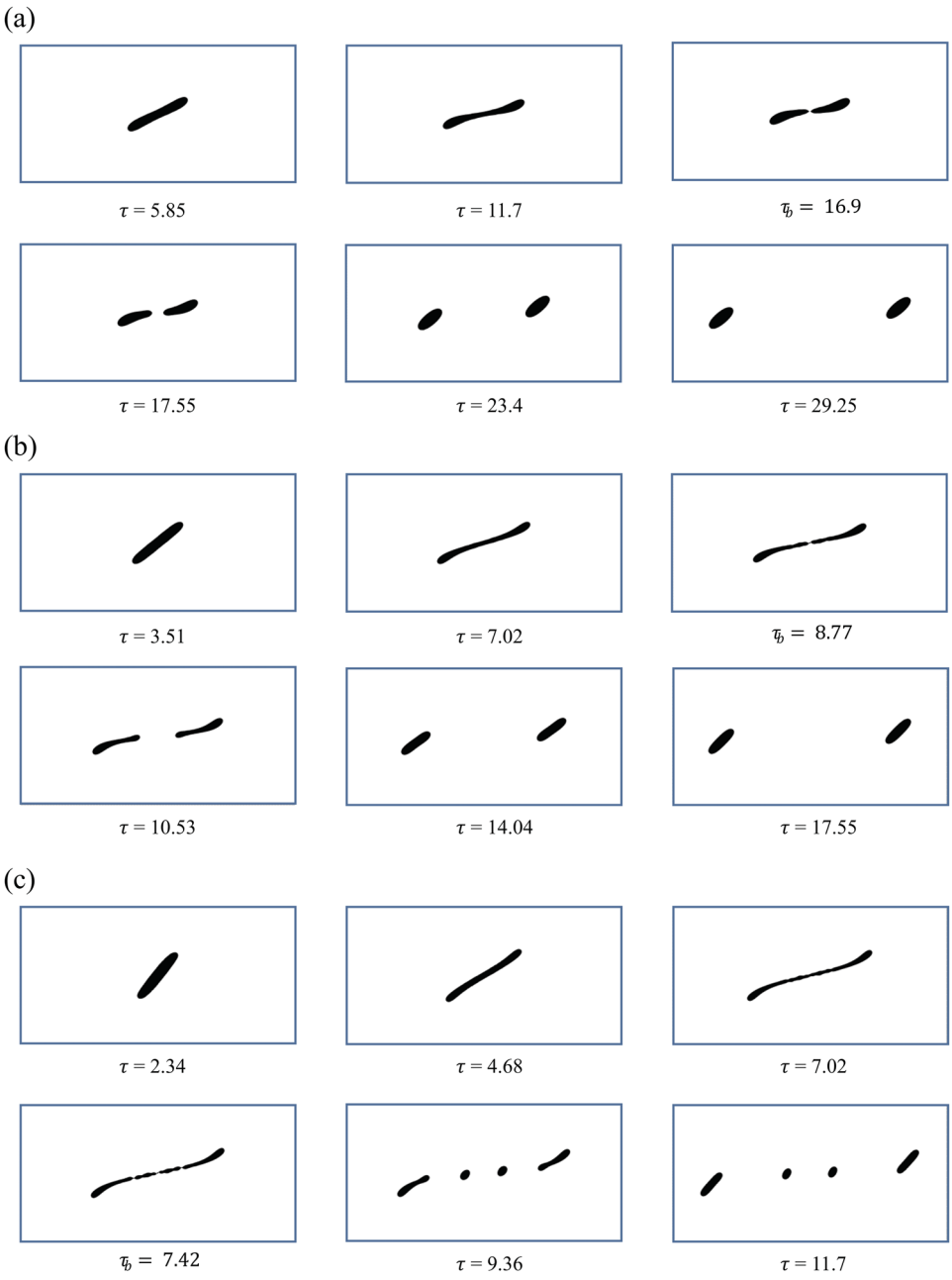

FIG. 7. Evolution of droplet breakup under the magnetic field effect in a simple shear flow at 90° (i.e., $\alpha = 90°$), Ca = 0.45, and $\lambda = 1$. (a) $Bo_m = 3.72$; (b) $Bo_m = 5.81$; and (c) $Bo_m = 8.38$.

the droplet along 45°, while, on the other hand, the magnetic field is acting along 135°, which is also the exact opposite direction to the favorable direction of the shear flow, thus resulting in a smaller deformation. Also, the outline of equilibrium droplet shapes is illustrated in Fig. 9(b), which confirms that with the increase in magnetic field strength, the droplet changes from an ellipsoidal shape to a spherical shape followed by a smaller deformation. Moreover, at $Bo_m = 8.38$ the magnetic field strength starts to orient the droplet along 135°, while for the other cases, the shear flow takes control of the orientation of the droplet.

Moreover, further simulations have been carried out at very high magnetic bond numbers (i.e., $Bo_m = 33.5$) along both $\alpha = 0°$ and 135° to investigate if the droplet breaks under extreme conditions, and interestingly, no breakup is observed in the computational domain even in these situations; instead, droplets with nearly pointed ends are generated, which also shows good agreement

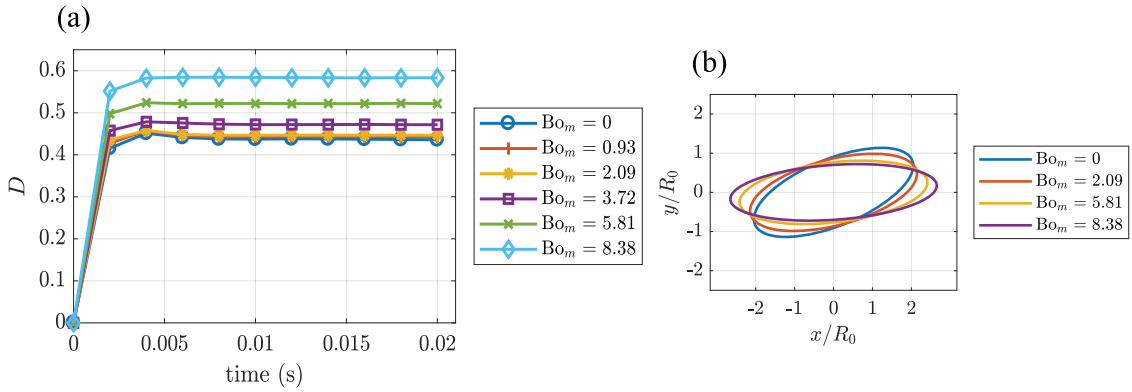

FIG. 8. Droplet under the effect of a magnetic field in a simple shear flow at 0° (i.e., α = 0°), Ca = 0.45, and λ = 1. (a) D vs time; (b) outline of equilibrium shapes at different magnetic bond numbers, Bo$_m$.

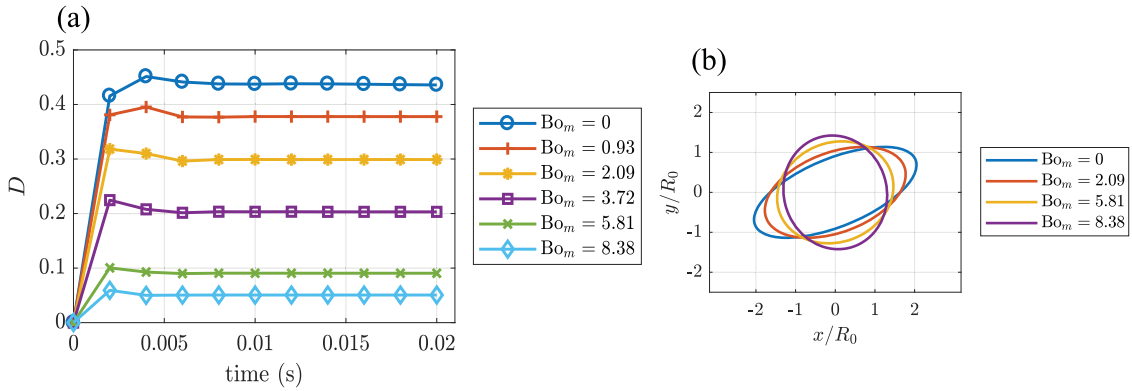

FIG. 9. Droplet under the effect of a magnetic field in a simple shear flow at 135° (i.e., α = 135°), Ca = 0.45, and λ = 1. (a) D vs time; (b) outline of equilibrium shapes at different magnetic bond numbers, Bo$_m$.

with the findings of Afkhami *et al.*[57] Overall, the results for different arbitrary directions suggest that it is possible to initiate droplet breakup in the Stokes flow regime by proper manipulation of a uniform magnetic field along 45° and 90°, while breakup can be suppressed by applying the magnetic field along both 0° and 135°.

C. Effect of the viscosity ratio on droplet breakup

In external flow conditions, viscosity ratio plays an important role on the dynamics of isolated drops in a shear flow, and from the experimental analyses of Grace[11] and Debruijn[10] it is found that the droplet reaches a steady state deformation up to a certain critical capillary number, Ca$_{cr}$, and above Ca$_{cr}$, the droplet keeps deforming until rupture occurs, which is also dependent on the viscosity ratio. Conversely, in particular, a detailed study on the critical droplet deformation D_{cr} at a low Reynolds number is missing in the literature. Here, in this section, we analyze the effect of the viscosity ratio on the droplet breakup phenomenon in the Stokes flow regime under a uniform magnetic field. Keeping the droplet size and capillary number fixed (i.e., Ca = 0.45), the magnetic field is applied along different directions for different viscosity ratios.

1. α = 45°

Figure 10 shows the effect of the viscosity ratio on the droplet breakup time under a uniform magnetic field at α = 45°. It can

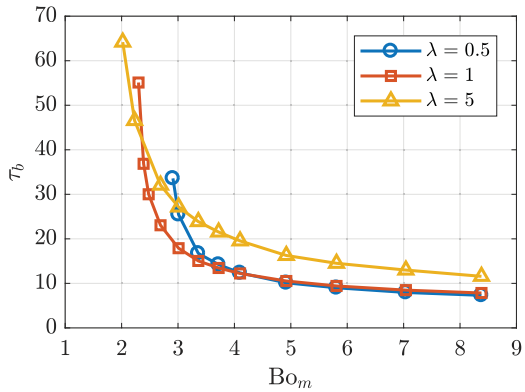

FIG. 10. Effect of the viscosity ratio on droplet breakup under a uniform magnetic field at α = 45° and Ca = 0.45. Droplet breakup time, τ_b vs Bo$_m$.

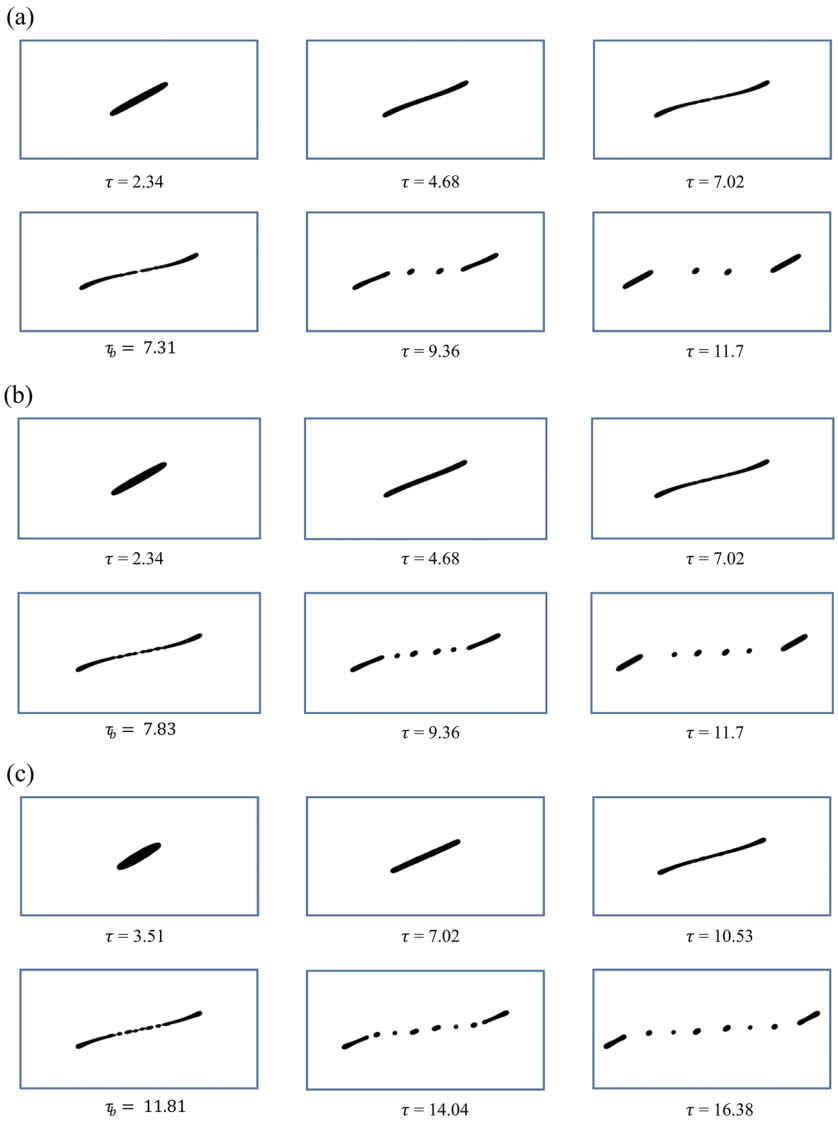

FIG. 11. Evolution of droplet breakup under a uniform magnetic field in a simple shear flow at 45° (i.e., $\alpha = 45°$), Ca = 0.45, and $\mathrm{Bo}_m = 8.38$. (a) $\lambda = 0.5$; (b) $\lambda = 1$; and (c) $\lambda = 5$.

be seen that at a fixed viscosity ratio, as the magnetic bond number Bo_m increases, the droplet rupture time decreases. Also, there exists a critical magnetic bond number, Bo_{cr}, for all viscosity ratios below which the droplet does not breakup anymore. Moreover, at a fixed magnetic bond number Bo_m, as the viscosity ratio increases, the breakup time increases, except when the magnetic bond number is near the critical magnetic bond number Bo_{cr}. This is because with the increase in viscosity ratios, the droplet shows more resistance to droplet deformation. As a result, it takes more time for a particular magnetic field strength to induce rupture to a more viscous droplet compared to a less viscous droplet. Interestingly, the critical magnetic bond number Bo_{cr} also decreases for more viscous droplets.

Figure 11 shows the evolution of droplet breakup under a magnetic field at $\alpha = 45°$ for different viscosity ratios. It can be seen that at a magnetic bond number $\mathrm{Bo}_m = 8.38$ for all viscosity ratios, the droplet goes through a similar kind of evolution from the

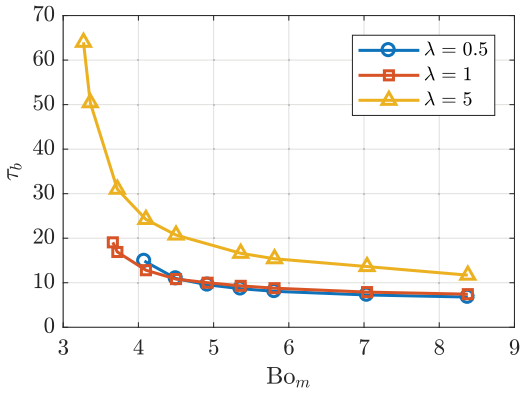

FIG. 12. Effect of the viscosity ratio on droplet breakup under a uniform magnetic field at $\alpha = 90°$ and Ca = 0.45. Droplet breakup time, τ_b vs Bo_m.

initial stage to the point where it ruptures, as discussed in Secs. IV B 1 and IV B 2; however, more necks appear near the center of the droplet due to the increased resistance toward droplet deformation with the increase in the viscosity ratios, which in turn give rise to more number of satellite droplets after the droplet disintegrates. Also, we observed the subsequent production of smaller and larger satellite droplets [Figs. 11(b) and 11(c)] followed by the formation of the largest daughter droplets by the first elongative end pinching during the droplet breakup process, which also agrees with the experimental findings of Marks. Furthermore, the size of the daughter droplets decreases with the increase in the viscosity ratio, due to the increased resistance to droplet deformation.

2. $\alpha = 90°$

Now, we apply the magnetic field in a direction perpendicular to the flow field (i.e., $\alpha = 90^{\circ}$) to investigate its effect on the droplet breakup phenomenon for different viscosity ratios. Figure 12 displays the relationship between the breakup time τ_b and the magnetic bond number Bo_m at three different viscosity ratios. Similar to the $\alpha = 45^{\circ}$ case mentioned above, in this case at a fixed viscosity ratio,

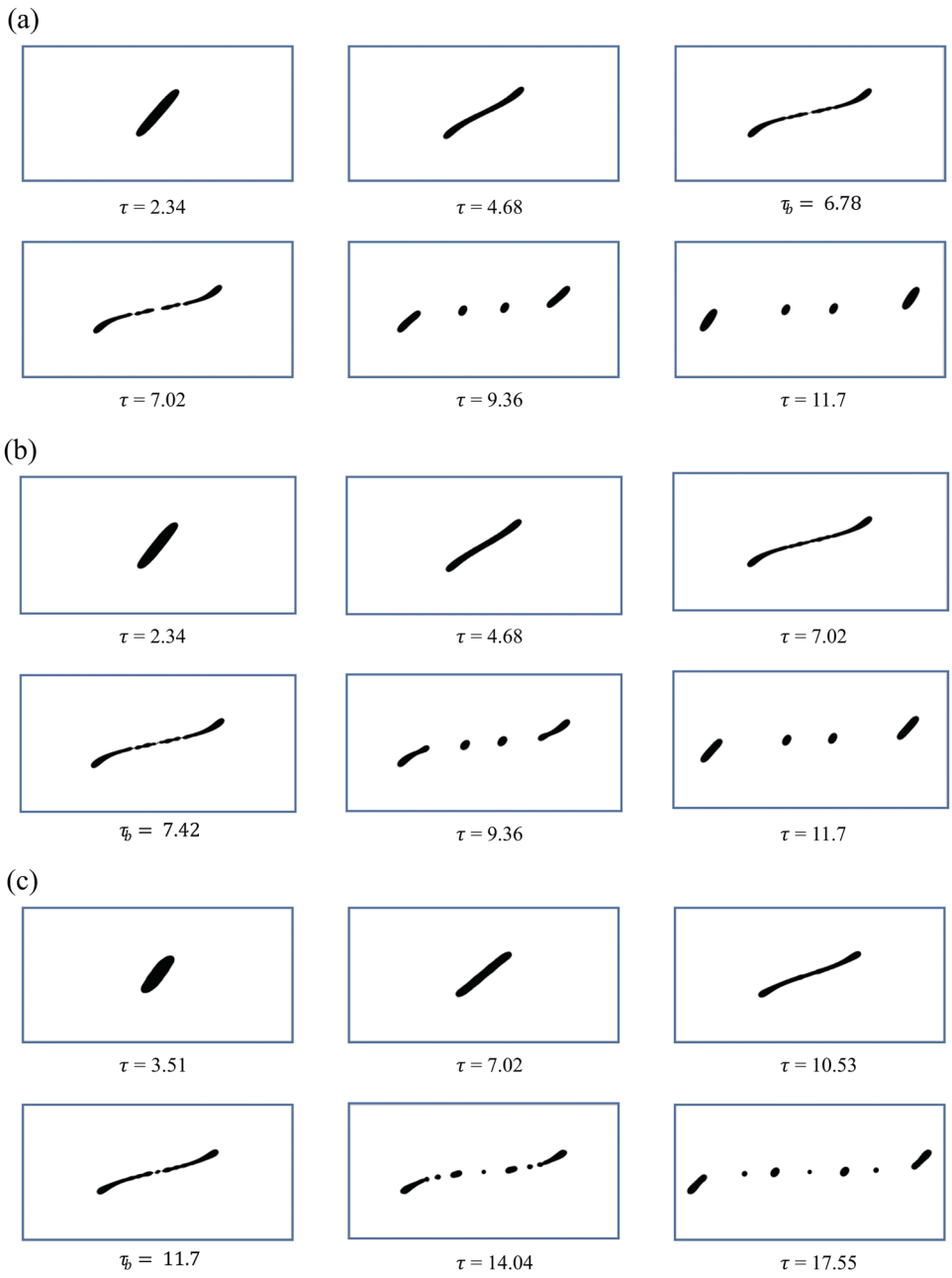

FIG. 13. Evolution of droplet breakup under a uniform magnetic field in a simple shear flow at 90° (i.e., $\alpha = 90°$), Ca = 0.45, and $Bo_m = 8.38$. (a) $\lambda = 0.5$; (b) $\lambda = 1$; and (c) $\lambda = 5$.

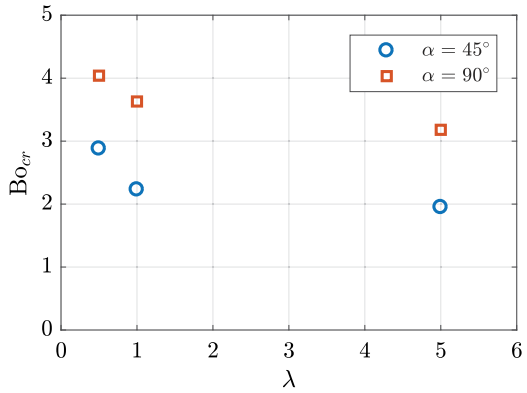

FIG. 14. Relationship between the critical magnetic bond number, Bo_{cr}, and viscosity ratio, λ, for different arbitrary magnetic field directions.

the droplet rupture time decreases with increasing the magnetic field strength. Also, a critical magnetic bond number, Bo_{cr}, exists for all viscosity ratios, which gradually decreases for more viscous droplets. Figure 13 shows the evolution of the droplet shape from the initial stage to the breakup stage under a uniform magnetic field at $\alpha = 90°$, and it can be seen that for all the cases, the droplet initially tends to orient itself along the direction of the magnetic field over time, followed by the transformation of the spherical droplet into a dumbbell shape with fixed diameter bulbs at both ends. Eventually, more necks are developed due to the shear and magnetic stresses acting along the interface near the center, which in turn give rise to multiple satellite droplets; however, at $\alpha = 90°$ we observed the production of smaller and larger satellite droplets only at a higher viscosity ratio (i.e., lambda = 5). Moreover, the size of the daughter droplets appears smaller at $\alpha = 90°$ compared to $\alpha = 45°$. Furthermore, at $\alpha = 90°$ as the viscosity ratio is increased beyond $\lambda \geq 1$, fewer satellite droplets are found in the computational domain compared to the number of satellite droplets that appear at $\alpha = 45°$.

Finally, the relationship between the critical magnetic bond number, Bo_{cr}, and the viscosity ratio, λ, for different directions is demonstrated in Fig. 14. It shows that at a fixed λ, the critical magnetic bond number Bo_{cr} always has a higher value at $\alpha = 90°$ than at $\alpha = 45°$. This is because the magnetic field additionally stretches the droplet along the flow direction at $\alpha = 45°$, which ultimately induces rupture in the droplet at a faster rate. As a result, the critical magnetic bond number Bo_{cr} appears earlier at $\alpha = 45°$ compared to $\alpha = 90°$, where we apply the magnetic field in a direction perpendicular to the flow domain.

3. $\alpha = 0°$

Figure 15 illustrates the effect of the viscosity ratio on droplet breakup under a uniform magnetic field at $\alpha = 0°$. From Fig. 15(a), it can be seen that at a fixed magnetic bond number Bo_m, the deformation of the droplet D decreases with the increase in the viscosity ratio. This is due to the fact that as the droplet becomes more viscous, it shows more resistance to deformation, which in turn results in a more spherical droplet shape. Interestingly, for a more viscous droplet (i.e., $\lambda = 5$) at a smaller magnetic field strength (i.e., $\mathrm{Bo}_m = 2.09$), we observed a rapid decline in deformation compared to less viscous droplets (i.e., $\lambda = 0.5$ and 1). Figure 15(b) depicts the outline of the final equilibrium droplet shapes at $\mathrm{Bo}_m = 2.09$, which also confirms that with the increase in viscosity ratio, the droplet tends to align itself more toward the direction of the magnetic field (i.e., orientation angle θ decreases).

4. $\alpha = 135°$

Finally, the magnetic field is applied along 135° to investigate its effect on droplet rheology at different viscosity ratios. From Fig. 16(a), it can be seen that, similar to the case mentioned above, the droplet deformation D decreases with the increase in the viscosity ratio. But in this case, at a particular magnetic field strength and viscosity ratio, the droplet deformation appears much smaller compared to the deformation at $\alpha = 0°$. The primary reason behind this could be attributed to the fact that at $\alpha = 135°$, the magnetic field induced deformation acts along the exact opposite direction of the shear induced deformation, i.e., deformation D decreases. Furthermore, the droplet aligns itself more toward the direction of the magnetic field with the increase in the viscosity ratio [Fig. 16(b)], which is also similar to the orientation trend observed at $\alpha = 0°$.

Overall, the results suggest that at Ca = 0.45, increasing the viscosity ratio along both $\alpha = 45°$ and 90° initiates a delayed breakup.

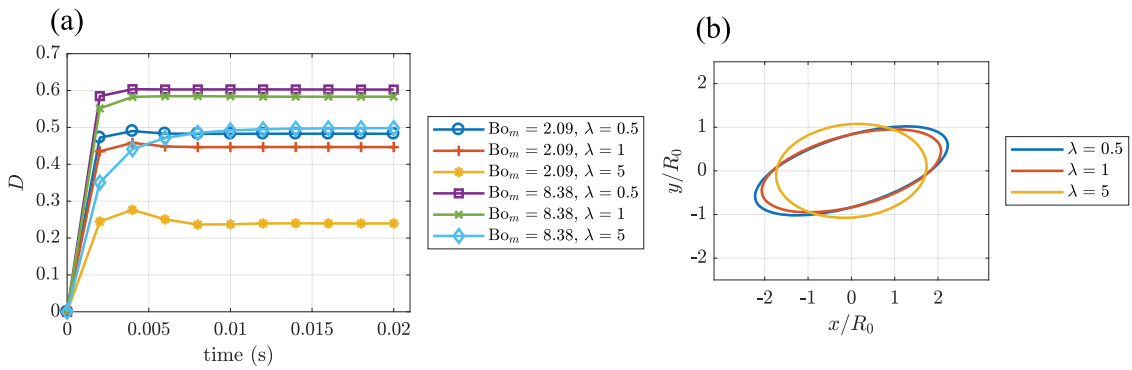

FIG. 15. Effect of the viscosity ratio on droplet deformation under a uniform magnetic field at $\alpha = 0°$ and Ca = 0.45. (a) D vs time; (b) outline of equilibrium shapes at $\mathrm{Bo}_m = 2.09$.

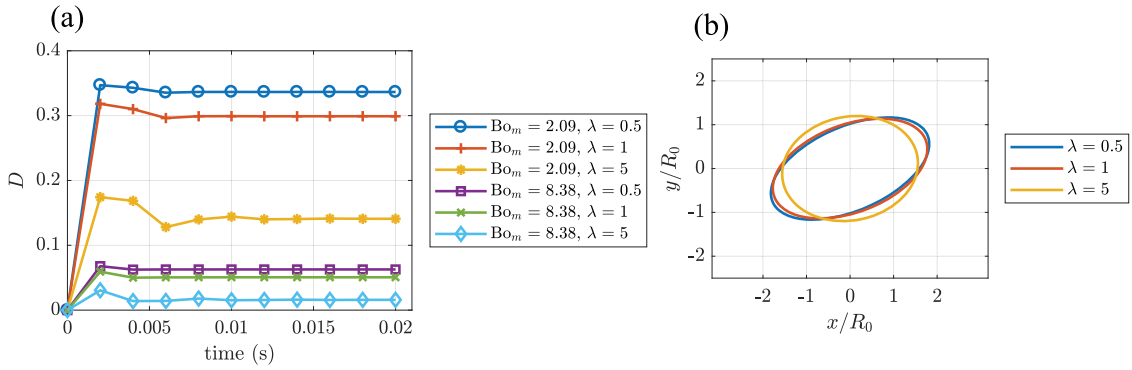

FIG. 16. Effect of the viscosity ratio on droplet deformation under a uniform magnetic field at $\alpha = 135°$ and Ca = 0.45. (a) D vs time; (b) outline of equilibrium shapes at $Bo_m = 2.09$.

At a fixed viscosity ratio, the critical magnetic bond number Bo_{cr} always has a higher value at $\alpha = 90°$ than at $\alpha = 45°$. On the other hand, at a specific magnetic field strength (i.e., $Bo_m = 2.09$), increasing the viscosity ratio along both $\alpha = 0°$ and 135° results in a smaller deformation; however, the deformation of the droplet along $\alpha = 135°$ is found comparatively smaller than the deformation at $\alpha = 0°$.

V. CONCLUSION

The breakup of a ferrofluid droplet in a simple shear flow under the influence of a uniform magnetic field along different directions at a low Reynolds number (i.e., Re = 0.03) is systematically studied in this paper. The results show that at a low capillary number (i.e., Ca ≤ 0.5), in the absence of any external forces, the droplet reaches a steady state deformation when suspended in another viscous medium in a shear flow; however, when a magnetic field is applied along 45° and 90°, the droplet starts to show unsteady behavior with the increase in magnetic field strength and eventually ruptures. We found that there exists a critical magnetic Bond number, Bo_{cr}, above which the droplet shows this behavior, which is also dependent on the direction of the magnetic field. For example, at $\alpha = 45°$, the magnitude of Bo_{cr} is found to be approximately 2.23 (i.e., $Bo_{cr}^{45°} \approx 2.23$), while at $\alpha = 90°$ it is found to be approximately 3.63 (i.e., $Bo_{cr}^{90°} \approx 3.63$). Also, as we increase the magnetic field strength beyond Bo_{cr} for both cases, the time to induce rupture in the droplet decreases. Moreover, for the same magnetic field strength, more satellite droplets are observed at $\alpha = 45°$ compared to $\alpha = 90°$. On the other hand, applying a magnetic field along 0° and 135° suppresses droplet breakup. Even at a higher magnetic field strength, a steady state deformation was observed in both cases.

Furthermore, we investigated the effect of viscosity ratios on the droplet breakup phenomenon under a uniform magnetic field at different directions and found that for both $\alpha = 45°$ and 90°, at a fixed magnetic bond number, the breakup time increases as the viscosity ratio λ increases, except when Bo_m is near the critical magnetic bond number Bo_{cr}. Also, the critical magnetic bond number Bo_{cr} decreases for a more viscous droplet. Additionally, with the increase in viscosity ratio at a fixed magnetic bond number, more satellite droplets are observed although, for the same Bo_m and λ, a larger number of satellite droplets are observed at $\alpha = 45°$ compared to 90°. Moreover, at a fixed λ, Bo_{cr} always has a higher value at $\alpha = 90°$ than at $\alpha = 45°$. Conversely, when the magnetic field is directed along 0° and 135°, at a particular magnetic field strength, the droplet deformation D decreases with an increase in viscosity ratio and the droplet tends to orient itself more toward the magnetic field direction. These findings indicate the enormous potential of magnetic fields as a useful tool for controlling breakup of ferrofluid droplets and emulsion rheology, which are relevant to a variety of applications in the fields of microfluidics, polymer processing, and chemical engineering.

ACKNOWLEDGMENTS

The authors gratefully acknowledge the financial support from the Department of Mechanical and Aerospace Engineering (MAE) and the Center for Biomedical Research (CBR) at Missouri University of Science and Technology.

REFERENCES

[1]D. J. McClements, *Food Emulsions: Principles, Practices, and Techniques* (CRC Press, 2015).
[2]F. Nielloud, *Pharmaceutical Emulsions and Suspensions: Revised and Expanded* (CRC Press, 2000).
[3]C. Han, *Multiphase Flow in Polymer Processing* (Elsevier, 2012).
[4]R. G. Larson, *The Structure and Rheology of Complex Fluids* (Oxford University Press, New York, 1999), Vol. 150.
[5]P. Garstecki, H. A. Stone, and G. M. Whitesides, "Mechanism for flow-rate controlled breakup in confined geometries: A route to monodisperse emulsions," Phys. Rev. Lett. **94**, 164501 (2005).
[6]A. Vananroye, P. Van Puyvelde, and P. Moldenaers, "Structure development in confined polymer blends: Steady-state shear flow and relaxation," Langmuir **22**, 2273–2280 (2006).
[7]M. Loewenberg and E. Hinch, "Numerical simulation of a concentrated emulsion in shear flow," J. Fluid Mech. **321**, 395–419 (1996).
[8]B. Bentley and L. G. Leal, "An experimental investigation of drop deformation and breakup in steady, two-dimensional linear flows," J. Fluid Mech. **167**, 241–283 (1986).
[9]K. Jansen, W. Agterof, and J. Mellema, "Droplet breakup in concentrated emulsions," J. Rheol. **45**, 227–236 (2001).
[10]R. A. Debruijn, "Deformation and breakup of drops in simple shear flows," Ph.D. thesis, Technische University, Eindhoven, The Netherlands, 1991.

[11]H. P. Grace, "Dispersion phenomena in high viscosity immiscible fluid systems and application of static mixers as dispersion devices in such systems," Chem. Eng. Commun. **14**, 225–277 (1982).
[12]F. Rumscheidt and S. Mason, "Particle motions in sheared suspensions XI. Internal circulation in fluid droplets (experimental)," J. Colloid Sci. **16**, 210–237 (1961).
[13]G. I. Taylor, "The viscosity of a fluid containing small drops of another fluid," Proc. R. Soc. London, Ser. A **138**, 41–48 (1932).
[14]G. I. Taylor, "The formation of emulsions in definable fields of flow," Proc. R. Soc. A **146**, 501–523 (1934).
[15]T. Mason and J. Bibette, "Shear rupturing of droplets in complex fluids," Langmuir **13**, 4600–4613 (1997).
[16]H. A. Stone, "Dynamics of drop deformation and breakup in viscous fluids," Annu. Rev. Fluid Mech. **26**, 65–102 (1994).
[17]Y. Fu, L. Bai, Y. Jin, and Y. Cheng, "Theoretical analysis and simulation of obstructed breakup of micro-droplet in T-junction under an asymmetric pressure difference," Phys. Fluids **29**, 032003 (2017).
[18]K. Feigl, A. Baniabedalruhman, F. X. Tanner, and E. J. Windhab, "Numerical simulations of the breakup of emulsion droplets inside a spraying nozzle," Phys. Fluids **28**, 123103 (2016).
[19]L. Scarbolo, F. Bianco, and A. Soldati, "Coalescence and breakup of large droplets in turbulent channel flow," Phys. Fluids **27**, 073302 (2015).
[20]J. Li, Y. Y. Renardy, and M. Renardy, "Numerical simulation of breakup of a viscous drop in simple shear flow through a volume-of-fluid method," Phys. Fluids **12**, 269–282 (2000).
[21]D. Barthes-Biesel and A. Acrivos, "Deformation and burst of a liquid droplet freely suspended in a linear shear field," J. Fluid Mech. **61**, 1–22 (1973).
[22]M. De Menech, "Modeling of droplet breakup in a microfluidic T-shaped junction with a phase-field model," Phys. Rev. E **73**, 031505 (2006).
[23]R. van der Sman and S. van der Graaf, "Emulsion droplet deformation and breakup with lattice Boltzmann model," Comput. Phys. Commun. **178**, 492–504 (2008).
[24]V. Sibillo, M. Simeone, and S. Guido, "Break-up of a Newtonian drop in a viscoelastic matrix under simple shear flow," Rheol. Acta **43**, 449–456 (2004).
[25]A. Vananroye, P. Van Puyvelde, and P. Moldenaers, "Effect of confinement on droplet breakup in sheared emulsions," Langmuir **22**, 3972–3974 (2006).
[26]P. Garstecki, M. J. Fuerstman, H. A. Stone, and G. M. Whitesides, "Formation of droplets and bubbles in a microfluidic T-junction–scaling and mechanism of break-up," Lab Chip **6**, 437–446 (2006).
[27]A. M. Leshansky and L. M. Pismen, "Breakup of drops in a microfluidic T junction," Phys. Fluids **21**, 023303 (2009).
[28]J. Sherwood, "Breakup of fluid droplets in electric and magnetic fields," J. Fluid Mech. **188**, 133–146 (1988).
[29]B. A. Jackson, K. J. Terhune, and L. B. King, "Ionic liquid ferrofluid interface deformation and spray onset under electric and magnetic stresses," Phys. Fluids **29**, 064105 (2017).
[30]G. I. Taylor, "Disintegration of water drops in an electric field," Proc. R. Soc. London, Ser. A **280**, 383–397 (1964).
[31]R. T. Collins, J. J. Jones, M. T. Harris, and O. A. Basaran, "Electrohydrodynamic tip streaming and emission of charged drops from liquid cones," Nat. Phys. **4**, 149 (2008).
[32]J. S. Eow and M. Ghadiri, "Motion, deformation and break-up of aqueous drops in oils under high electric field strengths," Chem. Eng. Process. **42**, 259–272 (2003).
[33]G. Katsikis, J. S. Cybulski, and M. Prakash, "Synchronous universal droplet logic and control," Nat. Phys. **11**, 588 (2015).
[34]D. R. Link, E. Grasland-Mongrain, A. Duri, F. Sarrazin, Z. Cheng, G. Cristobal, M. Marquez, and D. A. Weitz, "Electric control of droplets in microfluidic devices," Angew. Chem., Int. Ed. **45**, 2556–2560 (2006).
[35]A. Ahmed, B. A. Fleck, and P. R. Waghmare, "Maximum spreading of a ferrofluid droplet under the effect of magnetic field," Phys. Fluids **30**, 077102 (2018).
[36]O. T. Mefford, R. C. Woodward, J. D. Goff, T. Vadala, T. G. S. Pierre, J. P. Dailey, and J. S. Riffle, "Field-induced motion of ferrofluids through immiscible viscous media: Testbed for restorative treatment of retinal detachment," J. Magn. Magn. Mater. **311**, 347–353 (2007).
[37]S. Banerjee, M. Fasnacht, S. Garoff, and M. Widom, "Elongation of confined ferrofluid droplets under applied fields," Phys. Rev. E **60**, 4272 (1999).
[38]V. B. Varma, A. Ray, Z. M. Wang, Z. P. Wang, and R. V. Ramanujan, "Droplet merging on a lab-on-a-chip platform by uniform magnetic fields," Sci. Rep. **6**, 37671 (2016).
[39]V. B. Varma, "Development of magnetic structures by micro-magnetofluidic techniques," Ph.D. thesis, Nanyang Technological University, 2017.
[40]A. Ray, V. B. Varma, P. Jayaneel, N. Sudharsan, Z. Wang, and R. V. Ramanujan, "On demand manipulation of ferrofluid droplets by magnetic fields," Sens. Actuators, B **242**, 760–768 (2017).
[41]M. R. Hassan, J. Zhang, and C. Wang, "Deformation of a ferrofluid droplet in simple shear flows under uniform magnetic fields," Phys. Fluids **30**, 092002 (2018).
[42]J. Rallison, "The deformation of small viscous drops and bubbles in shear flows," Annu. Rev. Fluid Mech. **16**, 45–66 (1984).
[43]A. Acrivos, "The breakup of small drops and bubbles in shear flows," Ann. N. Y. Acad. Sci. **404**, 1–11 (1983).
[44]L. H. Cunha, I. R. Siqueira, T. F. Oliveira, and H. D. Ceniceros, "Field-induced control of ferrofluid emulsion rheology and droplet break-up in shear flows," Phys. Fluids **30**, 122110 (2018).
[45]L. Rosenfeld, T. Lin, R. Derda, and S. K. Tang, "Review and analysis of performance metrics of droplet microfluidics systems," Microfluid. Nanofluid. **16**, 921–939 (2014).
[46]T. M. Squires and S. R. Quake, "Microfluidics: Fluid physics at the nanoliter scale," Rev. Mod. Phys. **77**, 977 (2005).
[47]H. A. Stone, A. D. Stroock, and A. Ajdari, "Engineering flows in small devices: Microfluidics toward a lab-on-a-chip," Annu. Rev. Fluid Mech. **36**, 381–411 (2004).
[48]J. D. Tice, A. D. Lyon, and R. F. Ismagilov, "Effects of viscosity on droplet formation and mixing in microfluidic channels," Anal. Chim. Acta **507**, 73–77 (2004).
[49]M. T. Guo, A. Rotem, J. A. Heyman, and D. A. Weitz, "Droplet microfluidics for high-throughput biological assays," Lab Chip **12**, 2146–2155 (2012).
[50]D. Shi, Q. Bi, and R. Zhou, "Numerical simulation of a falling ferrofluid droplet in a uniform magnetic field by the Voset method," Numer. Heat Transfer, Part A **66**, 144–164 (2014).
[51]E. Olsson and G. Kreiss, "A conservative level set method for two phase flow," J. Comput. Phys. **210**(1), 225–246 (2005).
[52]R. E. Rosensweig, *Ferrohydrodynamics* (Cambridge University Press, 1985).
[53]J. A. Stratton, *Electromagnetic Theory* (John Wiley & Sons, 2007).
[54]S. Guido and M. Villone, "Three-dimensional shape of a drop under simple shear flow," J. Rheol. **42**, 395–415 (1998).
[55]M. Kennedy, C. Pozrikidis, and R. Skalak, "Motion and deformation of liquid drops, and the rheology of dilute emulsions in simple shear flow," Comput. Fluids **23**, 251–278 (1994).
[56]R. Cox, "The deformation of a drop in a general time-dependent fluid flow," J. Fluid Mech. **37**, 601–623 (1969).
[57]S. Afkhami, A. Tyler, Y. Renardy, M. Renardy, T. S. Pierre, R. Woodward, and J. Riffle, "Deformation of a hydrophobic ferrofluid droplet suspended in a viscous medium under uniform magnetic fields," J. Fluid Mech. **663**, 358–384 (2010).
[58]C. R. Marks, "Drop breakup and deformation in sudden onset strong flows," Ph.D. thesis, University of Maryland at College Park, 1998.